

Local magnetic ordering in $\text{La}_{1-x}\text{Ca}_x\text{MnO}_3$ determined by spin-polarized x-ray absorption spectroscopy

Q. Qian and T. A. Tyson^{a)}

Department of Physics, New Jersey Institute of Technology, Newark, New Jersey 07102

C.-C. Kao

Brookhaven National Laboratory, Upton, New York 11973

M. Croft

Department of Physics and Astronomy, Rutgers University, Piscataway, New Jersey 08854 and National Synchrotron Light Source, Brookhaven National Laboratory, Upton, NY 11973

A. Yu. Ignatov

Department of Physics, New Jersey Institute of Technology, Newark, New Jersey 07102

(Received 9 January 2002; accepted for publication 20 February 2002)

A systematic study of spin-dependent Mn *K*-edge x-ray absorption spectra was performed on $\text{La}_{1-x}\text{Ca}_x\text{MnO}_3$. By examining the changes in the pre-edge spectra with the temperature, a model of the excitation process is developed and used to predict the temperature dependent changes in the local magnetic ordering about Mn sites. The approach is of general applicability to perovskite systems. It can be used to determine the change in the local magnetic order (ferromagnetic versus antiferromagnetic) about a transition metal site upon going through a transition or as the result of external perturbations. © 2002 American Institute of Physics.

[DOI: 10.1063/1.1473700]

High temperature superconductivity, and more recently colossal magnetoresistance (CMR), phenomena have stimulated a far-reaching renaissance of perovskite based transition metal–oxide physics. There has been a symbiosis in this field among the evolving understanding of the electronic structure, a way by which to synthesize materials for tunability/control, and the experimental spectroscopies that probe it. X-ray absorption spectroscopy (XAS) and x-ray emission spectroscopy (XES) have both contributed to and benefited from this symbiosis in substantial ways.

In the case of CMR manganite materials Mn *K* XAS and XES have proved valuable in elucidating important variations in the Mn-*d* configuration, and in local Jahn–Teller distortion effects. Recently detailed high resolution XAS work by Bridges *et al.*¹ and by Qian *et al.*² have also provided evidence of intriguing temperature dependencies of the Mn *K* XAS pre-edges of $\text{La}_{1-x}\text{Ca}_x\text{MnO}_3$ materials which accompany changes upon crossing phase boundaries that involve combinations of insulating, paramagnetic, antiferromagnetic, ferromagnetic, and charge–orbital ordered phases. Heretofore, however, no clear proposal for understanding these interphase changes has been made. In this letter, we exploit a powerful combination of XAS and XES to extract spin-polarized x-ray absorption spectra and integrate the results into a spin-dependent excitation model which is sensitive to local magnetic order.

Spin-polarized x-ray absorption near-edge spectroscopy (SPXANES) is based on energy resolving the *3p* to *1s* transition (*K_β* emission) and measuring the emission from the main or satellite lines as a function of the incident x-ray energy. The initial measurements were performed by Härmäläinen *et al.*³ on MnO and MnF₂ and then extended to

other open-shell *3d* elements.^{2–7} Previous studies focused on the nature of the splitting between spin up and spin down channels in the main line. No emphasis was made on the pre-edge region and on the temperature dependant changes in SPXANES.

Samples of the $\text{La}_{1-x}\text{Ca}_x\text{MnO}_3$ series were synthesized and characterized by the procedure described in Ref. 8. Mn SPXANES measurements were performed at the National Synchrotron Light Source's (NSLS) 27 pole wiggler Beamline X21A. Experimental details of them are described elsewhere.^{2,9,10} SPXANES spectra were collected by monitoring the *K_β* fluorescence yield at two energies (*E*₁, centered on the satellite line, and *E*₂, centered 0.5 eV above the main peak,^{2,7} for a given *x*) specific to spin up and spin down final states while the incident energy across the near-edge

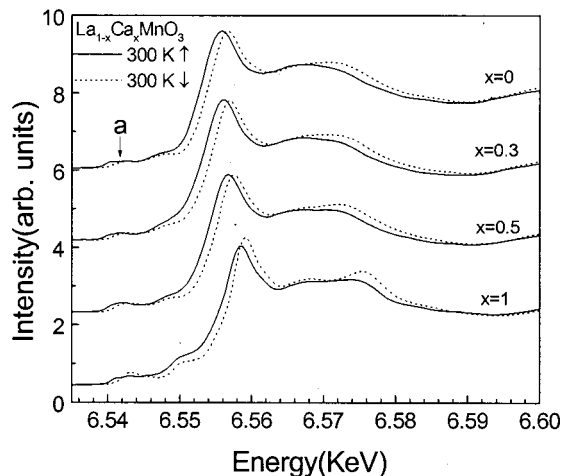


FIG. 1. SPXANES spectra of $\text{La}_{1-x}\text{Ca}_x\text{MnO}_3$. The solid (dotted) line corresponds to the spin up (down) channel measured at 300 K.

^{a)}Electronic mail: tyson@adm.njit.edu

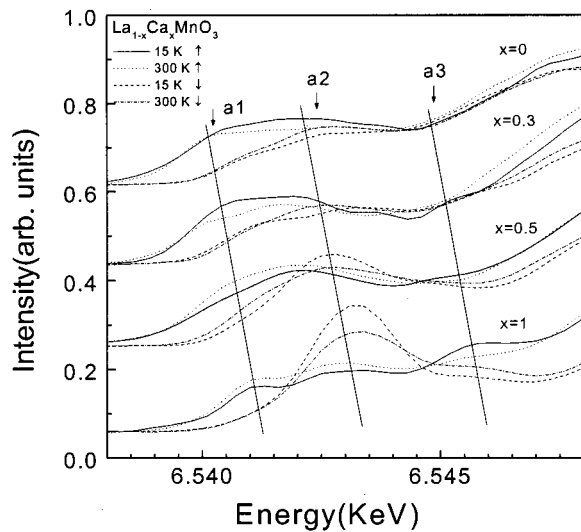


FIG. 2. Temperature dependent pre-edge SPXANES spectra of the region near feature *a* in Fig. 1. The three straight lines indicate the *a*1, *a*2, and *a*3 features.

region was scanned. Measurements were performed for $x = 0, 0.3, 0.5,$ and 1 at two temperatures, 15 and 300 K.

All the *K*-edge SPXANES spectra of $\text{La}_{1-x}\text{Ca}_x\text{MnO}_3$ are shown in Fig. 1. Notice the marked splitting between the spin up and spin down channels of both the main edges ($E \sim 6.55\text{--}6.58$ keV) and the pre-edges ($E \sim 6.535\text{--}6.55$ keV). Splitting of the main edge is primarily from exchange interaction of the photoelectron with the spin up and spin down densities of states. Details of the temperature dependence of the main edge feature in $\text{La}_{1-x}\text{Ca}_x\text{MnO}_3$ over the whole doping range will be discussed at length in a future article.⁹ In this letter we focus on the pre-edge region labeled *a*.

In Fig. 2 we expand the pre-edge region (*a* in Fig. 1) of the SPXANES spectra and three peaks (labeled *a*1, *a*2, and *a*3) in $\text{La}_{1-x}\text{Ca}_x\text{MnO}_3$ ($x = 0, 0.3, 0.5,$ and 1) are observed. Measurements were made above and below the temperatures of magnetic ordering. Note the significant temperature and spin dependence of the pre-edge spectra. We first point out that these features cannot originate from on-site direct quadrupole absorption, since the intensity of such transitions would be quite low (see Ref. 11). Elfimov *et al.*¹² and Bridges *et al.*¹ suggested that this structure might come from Mn $4p$ hybridization with the neighboring Mn $3d$ (see Fig. 5 in Ref. 1). In this simple physical picture, the Mn $1s$ electron can undergo a transition to final states formed by hybridization of an on-site Mn $4p$ and neighboring Mn $3d$ orbitals. In our model, we make the further assumption that the $1s$ to t_{2g} transition intensity vanishes. This is due to the fact that the $\text{La}_{1-x}\text{Ca}_x\text{MnO}_3$ system exhibits orbital ordering over a broad range of x .¹³ Both embedded cluster calculations¹⁴ and local density approximation (LDA) calculations¹⁵ predict no t_{2g} contribution to the Mn *K*-edge XAS spectra. Moreover, multiple scattering XANES calculations of a series of model systems with varying *d*-occupation numbers ($\text{CaO}_3, \text{A} = \text{Ti, Mn, Ni, Zn, Ge}$) are consistent with these results.¹⁰

Based on these assumptions, we have developed an electron excitation model with spin conservation (without t_{2g} final states) in order to understand the origin of the pre-edge

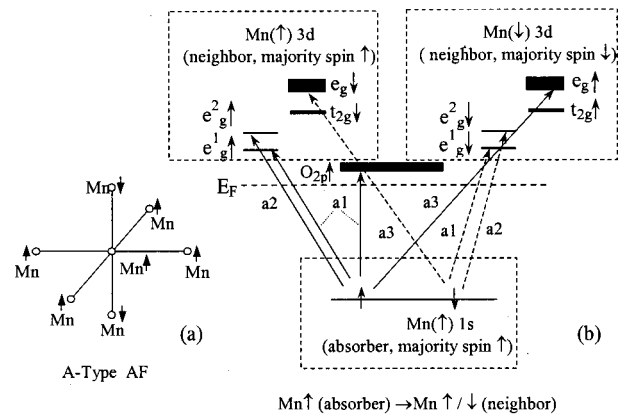


FIG. 3. Schematic diagram showing the transitions in the pre-edge for spin polarized absorption of A-type AF LaMnO_3 in the magnetically ordered state. (a) Local magnetic ordering of Mn ions (the O atoms are not shown for clarity). (b) Allowed transitions for excitation of Mn in which the *d* final state of a neighbor is of the same spin polarization as the absorber (left panel) as well as the case in which the spin polarization is reversed (right panel), respectively.

features *a*1, *a*2, and *a*3 (see Fig. 3). We start with LaMnO_3 which is an A-type antiferromagnet (AF) (see Refs. 16 and 17) below $T_N \sim 130$ K.¹³ Below T_N , each Mn ion is surrounded by four Mn ions (through oxygen) with the majority spin parallel and two Mn atoms with the majority spin antiparallel to the central Mn majority spin, as shown in Fig. 3(a).

In Fig. 3(b) we display our transition model which is based on dipole transitions (Mn $4p$ hybridized with the neighboring Mn e_g and O p). There are three boxes denoted by dashed lines, the lower one represents the center absorbing Mn site, defined as majority spin up (\uparrow). The upper left box corresponds to a neighboring Mn site with majority spin up (\uparrow), and the upper right box represents a neighboring Mn site with majority spin down (\downarrow). In Fig. 3(b), the absorber spin up Mn $1s$ (\uparrow) electron can make a transition to local majority spin orbitals e_g (\uparrow) of the neighboring Mn (\uparrow) (in the left upper box) with the same spin alignment as the absorber (density of state computations reveal holes in the majority e_g^1 band due to covalency⁹), and also to local minority spin orbitals e_g (\uparrow) of the neighboring Mn (\downarrow) (in the right upper box) with antiparallel spin alignment with respect to the absorber. Notice in the case of the Mn (\downarrow) neighbor, the local majority spin e_g orbital is labeled e_g (\downarrow), as shown in the right upper box in Fig. 3(b). The O $2p$ spin up channel transition in Fig. 3(b) is also possible due to hybridization with the Mn $4p$. Evidence of O $2p$ holes in LaMnO_3 was also found in optical measurements performed by Ju *et al.*¹⁸ All the long solid arrows correspond to the spin up transition channels in the SPXANES pre-edge region, while the long dashed arrows give the spin down transition channels. Labels *a*1, *a*2, and *a*3 refer to pre-edge *a* features in Fig. 2.

Now let us turn to the temperature dependence of our pre-edge SPXANES spectra. LaMnO_3 is an A-type AF at 15 K and is paramagnetic at 300 K. Crossing the T_N , upon warming changes the Mn majority spins alignment causing them to become randomly distributed, thereby changing the number of ferromagnetically aligned Mn neighbors from four to an average of three. This must enhance the transitions

shown in Fig. 3(b) (in the upper right box) and reduce those in Fig. 3(b) (in the upper left box). Therefore, for the spin up absorption channel, the $a1$ and $a2$ intensities should decrease, whereas the $a3$ intensity should increase. The temperature dependence of the spin down channel is expected to be reversed. This is what is observed experimentally for $a2$ feature in Fig. 2. Unfortunately, all but the $a3$ feature in CaMnO_3 are broad and hence the temperature dependent changes are difficult to ascertain. Weak suppression of the $a1$ spin up peak (Fig. 2) is caused by contributions from O p (\uparrow) that is enhanced with increased temperature. The $a1$ (\downarrow) is weaker than $a1$ (\uparrow) because there are no O p (\downarrow) states just above the Fermi level.

For the system with $x=0.3$, which becomes ferromagnetic at low temperature ($T_C \sim 250$ K),¹³ trends are observed that are similar to those found in the parent LaMnO_3 . One exception is that due to delocalization of the majority spin e_g^1 electron (seen as an increase in conductivity) the $a1$ feature increases. Further enhancement of this $a1$ feature is caused by an increase of O $2p$ holes due to increased covalency at low temperatures.² Interestingly, in the low temperature spin down measurement, the $a1$ and $a2$ features (expected for AF coupling only) are observed. This observation is not easy to reconcile with the results of neutron diffraction refinements, which provide a picture of long range ferromagnetic ordering. The spin down $a1$ and $a2$ intensities at low temperature may originate from antiparallel neighbors that exist below T_C , possibly due to FM and AF phase separation as was suggested initially by Wollan and Koehler¹⁹ and more recently by Moreo *et al.*²⁰

The $x=0.5$ system exhibits C-type AF order (below $T_N \sim 150$ K)¹³ in which each Mn ion has four neighboring Mn ions with antiparallel spin and two neighbors with parallel spin. It is then expected that the temperature dependence should be reversed compared to in the $x=0$ system. At low temperature (below the charge-ordering temperature, $T_{co} \sim 150$ K = T_N),¹³ the system is less covalent² so O $2p$ holes are delocalized. On the other hand, the majority spin e_g^1 conduction band electrons are localized as seen from the observed increase in resistivity (exponential dependence on temperature)²¹ at low temperature. Hence, due to the enhanced occupancy of the O $2p$ and majority spin e_g^1 states, the $a1$ feature is reduced at low temperature in accordance with our model, as observed.

CaMnO_3 is thought to be a G-type AF (below $T_N \sim 125$ K)¹³ where each Mn ion has six antiparallel Mn neighbors. The large $a1$ spin up peak is assigned to the unoccupied O $2p$ (\uparrow) states. Band structure computations have shown that ferromagnetic ordering of CaMnO_3 produces a split in the O $2p$ band with a broad spin up component near the Fermi level.⁹ It is possible that CaMnO_3 is a two phase material composed of FM and G-type AF (dominant) regions. It is known that CaMnO_3 has a small net magnetization²² which has previously been attributed to defects. The low intensity in the $a1$ peak at 15 K is due to a reduction in the covalency of CaMnO_3 below T_N .² No transition to O $2p$ (\downarrow) is observed in the $a1$ region in spin down spectra for the reason given above. The origin of the low

temperature $a2$ peak in the spin up spectrum can be understood as resulting from transitions on Mn sites within the FM ordered regions (discussed above). Hence, the temperature dependent behavior of the SPXANES spectra of CaMnO_3 with the exception of $a1$ is expected to mimic that of $x=0.5$.

We have shown that the changes in the pre-edge region with the temperature can be directly linked to changes in the local magnetic ordering of Mn ions around absorbing Mn sites. One can distinguish between a transition from a random local magnetic arrangement to an ordered arrangement such as AF (for example, A type, C type, or G type) or FM. This method has potential applicability for a wide range of perovskite transition metal systems or more generally for octahedrally coordinated transition metal systems.

Data acquisition was performed at Brookhaven National Laboratory's National Synchrotron Light Source which is funded by the U.S. Department of Energy Grant DE-AC02-98CH10886. This work was supported by Department of Energy, Office of Basic Energy Sciences, Grant No. DE-FG02-97ER45665. The authors are indebted to M. Greenblatt and S.-W. Cheong of Rutgers University for sample preparation. They also thank G. A. Sawatzky of the University of Groningen, The Netherlands, for helpful discussions.

¹F. Bridges, C. H. Booth, G. H. Kwei, J. J. Neumeier, and G. A. Sawatzky, *Phys. Rev. B* **61**, R9237 (2000).

²Q. Qian, T. A. Tyson, C.-C. Kao, M. Croft, S.-W. Cheong, and M. Greenblatt, *Phys. Rev. B* **62**, 13472 (2000).

³K. Hämäläinen, C.-C. Kao, J. B. Hastings, D. P. Siddons, L. E. Berman, V. Stojanoff, and S. P. Cramer, *Phys. Rev. B* **46**, 14274 (1992).

⁴F. M. F. de Groot, S. Pizzini, A. Fontaine, K. Hämäläinen, C.-C. Kao, and J. B. Hastings, *Phys. Rev. B* **51**, 1045 (1995).

⁵G. Peng, F. M. F. de Groot, K. Hämäläinen, J. A. Moore, X. Wang, M. M. Grush, J. B. Hastings, D. P. Siddons, W. H. Armstrong, O. C. Mullins, and S. P. Cramer, *J. Am. Chem. Soc.* **116**, 2914 (1994).

⁶X. Wang, F. M. F. de Groot, and S. P. Cramer, *Phys. Rev. B* **56**, 4553 (1997).

⁷T. A. Tyson, Q. Qian, C.-C. Kao, J.-P. Rueff, F. M. F. de Groot, M. Croft, S.-W. Cheong, M. Greenblatt, and M. A. Subramanian, *Phys. Rev. B* **60**, 4665 (1999).

⁸M. Croft, D. Sills, M. Greenblatt, C. Lee, S.-W. Cheong, K. V. Ramanujachary, and D. Tran, *Phys. Rev. B* **55**, 8726 (1997).

⁹Q. Qian, T. A. Tyson, S. Savrassov, C.-C. Kao, and M. Croft (unpublished).

¹⁰Q. Qian and T. A. Tyson (unpublished).

¹¹Q. Qian, T. A. Tyson, C.-C. Kao, M. Croft, S.-W. Cheong, G. Popov, and M. Greenblatt, *Phys. Rev. B* **64**, 024430 (2001).

¹²I. S. Elfimov, V. I. Anisimov, and G. A. Sawatzky, *Phys. Rev. Lett.* **82**, 4264 (1999).

¹³S.-W. Cheong and H. Y. Hwang, *Colossal Magnetoresistance Oxides*, edited by Y. Tokura (Gordon and Breach, Abingdon, UK, 2000).

¹⁴L. Hozoi, A. H. de Vries, and R. Broer, *Phys. Rev. B* **64**, 165104 (2001).

¹⁵M. Takahashi, J.-I. Igarashia, and P. Fulde, *J. Phys. Soc. Jpn.* **69**, 1614 (2000).

¹⁶J. B. Goodenough, *Phys. Rev.* **100**, 564 (1955).

¹⁷T. Hotta, S. Yunoki, M. Mayr, and E. Dagotto, *Phys. Rev. B* **60**, 15009 (1999).

¹⁸H. L. Ju, H.-C. Sohn, and K. M. Krishnan, *Phys. Rev. Lett.* **79**, 3230 (1997).

¹⁹E. O. Wollan and W. C. Koehler, *Phys. Rev.* **100**, 545 (1955).

²⁰A. Moreo, S. Yunoki, and E. Dagotto, *Science* **283**, 2034 (1999).

²¹G. P. Radaelli, D. E. Cox, M. Marezio, S.-W. Cheong, P. E. Schieffer, and A. P. Ramirez, *Phys. Rev. Lett.* **75**, 4484 (1995).

²²J. J. Neumeier and J. L. Cohn, *Phys. Rev. B* **61**, 14319 (2000).